JOURNAL OF MODERN OPTICS, 1997, VOL. 44, NO. 1, 127–148

Characterization of the human visual system threshold performance by a weighting function in the Gabor domain

J. MALO, A. M. PONS, A. FELIPE and J. M. ARTIGAS
Departamento Interuniversitario de Óptica, Facultat de Física, Universitat de València, C/Dr. Moliner 50, 46100 Burjassot, València, Spain. e-mail: Jesus.Malo@uv.es

(*Received 2 February 1996; revision received 28 May 1996*)

Abstract. As evidenced by many physiological and psychophysical reports, the receptive fields of the first-stage set of mechanisms of the visual process fit to two-dimensional (2D) compactly supported harmonic functions. The application of this set of band-pass filter functions to the input signal implies that the visual system carries out some kind of conjoint space/spatial frequency transform. Assuming that a conjoint transform is carried out, we present in this paper a new characterization of the visual system performance by means of a weighting function in the conjoint domain. We have called this weighting function (in the particular case of the Gabor transform) the Gabor stimuli Sensitivity Function (GSF) by analogy with the usually employed weighting function in the Fourier domain: the Contrast Sensitivity Function (CSF). An analytic procedure to obtain this conjoint weighting function from the psychophysical measurements of the CSF is derived. The accuracy of the procedure is proved showing the equivalence between some experimental Fourier weighting functions (2D CSFs), and the corresponding GSFs. The main advantage of this new characterization is that a weighting function in a space/spatial frequency domain can account for spatially variant behaviour, which cannot be included in a unique CSF, so a single GSF would be needed to include extra-foveal and large eccentricity behaviour. One example is given of how non-homogeneous systems can be easily characterized in this way.

1. Introduction

Among the main research objectives in the field of spatial vision, there is the implementation of algorithms for visual information encoding which, in accordance with physiology, could reduce the signal volume for the next processing stage. The strong correlation between luminance values in neighbouring points of the natural images [1] points to performing the information processing in a domain different from the spatial one [2, 3]. In this way, one of the tasks of the visual system must be to transform the input images, by projecting them over a more appropriate domain for their analysis.

Since the publication of the paper by Campbell and Green on contrast sensitivity to sinusoidal gratings [4], the visual system has been commonly characterized by accepting that it performs a Fourier transform (FT) of the input signal and, subsequently, the FT's coefficients are selectively attenuated by a weighting function defined in the spatial frequency domain: the CSF. In the 1980s several physiological studies [5–7] showed that the receptive fields of the cortical cells resemble compactly supported harmonic functions. At the same time, the

0950–0340/97 $12·00 © 1997 Taylor & Francis Ltd.

interest on the intrinsic two-dimensionality of the visual process led Daugman [8, 9] to question the frequency/orientation separability of the spatial vision mechanisms. In these pioneering works [8, 9], limited band-pass Gabor filter functions are proposed to characterize the receptive field and the spectral response of the mechanisms. Detailed 2D-oriented psychophysical measurements carried out by Daugman [10] and subsequently confirmed by Harvey and Doan [11] prove that in the initial stages of the visual process, the input signal is analysed by a set of filters simultaneously localized in the spatial and the frequency domains.

Since then, the papers of Daugman [12, 13], Porat and Zeevi [14], Field [3, 15], and Watson [16–18], among others, develop models where the analysing transform is no longer a Fourier transform, but some kind of conjoint space/spatial frequency transform more consistent with the experimental evidences. All these models describe different linear conjoint transforms (CT) applied by the system to place the signal into a more suitable domain for its analysis, but, in fact, these transforms can be considered as simple changes of domain, giving no clue about the real information process carried out by the system.

In this work we characterize these information reduction processes by means of a weighting function defined in the domain of the conjoint transform (CT). This weighting function acts on the coefficients of the CT just as the CSF acts on the coefficients of the FT. So, assuming that the system performs a generic linear CT as described in the literature, our contribution is focused in the following points:

- The description of the information reduction processes by a weighting function in a 4D space–frequency conjoint domain.
- To propose an analytic procedure to obtain the values of this 4D weighting function from the psychophysical data of the equivalent weighting function in the 2D Fourier domain (the 2D CSF).
- To test the proposed algorithm with experimental 2D CSF data.
- To emphasize, with a how-to example, the potentialities of this characterization to include in a single function a spatially variant behaviour, what is not possible in a Fourier characterization.

Finally, we want to point out that even though we have assumed the generic CT to be a Gabor transform (GT), it is not our objective to elucidate whether the Gabor transform is in fact the linear transform carried out by the visual system. This matter is still in discussion [19]. Anyway, the mathematical reasonings are completely generalizable to any other kind of linear conjoint transform, by changing GT for CT in the expressions.

2. Space–frequency analysis as an alternative to Fourier frequency analysis in the spatial vision field

We shall begin by remembering the basic ideas about space–frequency analysis and its advantages over Fourier frequency analysis.

In the contrast range where system behaviour is approximately linear, it is accepted that the system performs a transformation of the topographical signal $f(\mathbf{x})$ in such a way that $f(\mathbf{x})$ is then written as a linear combination (either continuous or discrete) of a set of base functions $\{g(\mathbf{x}, \mathbf{p})\}$ which are dependent on a parameter (or parameters) $\mathbf{p}$. That is:

$$f(\mathbf{x}) = \int_P C(\mathbf{p}) g(\mathbf{x}, \mathbf{p})\, d\mathbf{p}, \tag{1}$$

where the coefficients $C(\mathbf{p})$ indicate the participation degree of each $g(\mathbf{x}, \mathbf{p})$ function in the signal $f(\mathbf{x})$ or, in other words, to what extent the signal contains the characteristics of each base function.

The different approximations to space–frequency analysis (wavelet analysis [20–24], Gabor analysis [25] ...) have a common property which makes them different from Fourier analysis: the simultaneous localization of the base functions $g(\mathbf{x}, \mathbf{p})$ in the space and frequency domains. Thus, the coefficients $C(\mathbf{p})$ give information about $f(\mathbf{x})$ in both domains.

Within the space–frequency analysis, the method of obtaining the base functions and their analytical expressions constitute the main difference between the various approaches. In wavelet analysis, the set of base functions is obtained from one single generating function by expansions, compressions, translations and rotations [20, 23]. The elegance of this method has a drawback: the nonexistence of an explicit analytical expression for calculating the generating function. The kind of functions that can be considered as generating ones are limited by some theorems [22].

In the Gabor analysis the base is formed by harmonic functions of frequency $\mathbf{k}_0$ which are modulated by a Gaussian window centred in any point $\mathbf{x}_0$ of the spatial domain [25]:

$$g(\mathbf{x}, \mathbf{p}) = g(\mathbf{x}, \mathbf{x}_0, \mathbf{k}_0) = C \exp\left[-\left(\frac{\mathbf{x} - \mathbf{x}_0}{a}\right)^2\right] \exp -i\mathbf{k}_0\mathbf{x}. \tag{2}$$

Here C is just a constant to make $|g(\mathbf{x}, \mathbf{x}_0, \mathbf{k}_0)| = 1$. The Gaussian envelope, thanks to the simplicity of its analytic expression, allows a simultaneous and intuitive control of the shape of the function and its spectrum by adjusting the parameters of its formula [12]. Moreover, the Gabor function displays two fundamental properties: it makes possible parallel treatments in both frequency and space domains [26], and it minimizes the product of the widths in the space and frequency domains [12, 27]; thereby, the information supplied by each coefficient is maximal.

The advantages of space–frequency analysis are basically three:

(1) The image analysis from the coefficients of either its wavelet transform (WT) or Gabor transform (GT) facilitates the high-level process task. This is due to the fact that it is possible to assign a spatial and frequency significance to each coefficient (of either WT or GT).
(2) In either a hardware or neural implementation of the space–frequency transformations, the number of connections between pixels is minimized. This fact is due to the control of the spatial width as a function of the central frequency of each base function, which minimizes the image portion employed in calculating each coefficient [22]. On the contrary, in an FT, every image point must be employed in calculating each coefficient.
(3) Strong compression factors of natural images are obtained through the space–frequency representations [3, 13, 28–30]. The particular statistic of

these images leads to the fact that very few coefficients reach significant values, dramatically reducing the transformed function volume.

The introduction of this kind of analysis in the spatial vision field is due to two reasons; on the one hand, to the recognition of its intrinsic advantages over the Fourier analysis [3, 9, 13] and, on the other hand, to the physiological [5–7] and psychophysical [10, 11] evidences which indicate that the Gabor functions are the best fitting for receptive fields and frequency tuning mechanisms.

Criteria mentioned before have favoured the employment of this representation as a model for spatial vision [4, 31, 32] and for texture perception [31, 33] as well as the employment of Gabor stimuli in psychophysical experiments to study the interaction between the different mechanisms of detection in pattern recognition [15], or the induction and masking effects [34].

3. Gabor stimuli Sensitivity Function (GSF)

Assuming that the visual system has performed a GT of the input image, there exist two possibilities for explaining the information reduction which takes place during the processing. One possibility consists in proposing that the transformation is achieved by means of an incomplete basis and, therefore, when the image is decomposed with regard to such a basis there is a loss of information. The problem with this option is that the choice of the basis is decisive to obtain a suitable characterization, but establishing a criterion to adjust the parameters of each base function is not an easy task. The other possibility is to assume that the GT achieved is complete (or quasi-complete [26]), so the loss of information is placed in a selective weighting process after the transformation. This is the approach we have followed. In this case, the choice of the base becomes less critical, since the problem is now the calculation of the weights. This calculation, as we will see, can be formulated independently of the base selected.

We have called the Gabor stimuli Sensitivity Function (GSF) the weighting function acting on the GT coefficients, in the visual system case. This model of the encoding and initial filtering can be summarized in the block diagram shown in figure 1.

Linear behaviour of the system is required, as in the Fourier [35] case, since the GT and the weighting process after it are linear. Therefore, the model validity is, at first, limited to the low-contrast range. Nevertheless, the characterization of a system in the Gabor domain is less restrictive than the Fourier one, since system homogeneity is not an indispensable requirement here, as it is in the Fourier formalism due to the global character of the FT.

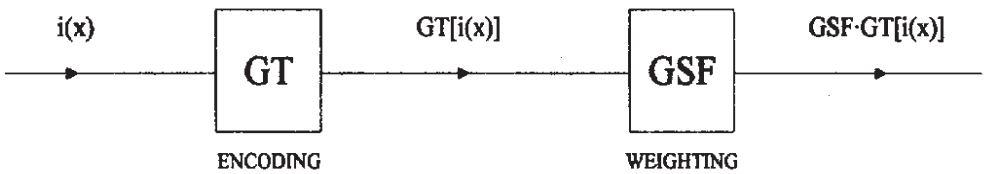

Figure 1. Block diagram of the transformations of the input signal (a still achromatic image) to obtain its distorted representation at cortex level (as a set of neural impulses of cells with Gabor-like receptive fields). The weighting function GSF includes both optical and neural degradation processes.

4. Relation between the weighting functions defined in the Fourier and Gabor domains

To establish the relation between both functions, we assume the equivalence of both system characterizations. That is, the same degraded image should be obtained if it were reconstructed from the output coefficients of either case. This is shown schematically in figure 2 and represented mathematically as

$$i'_{CSF}(\mathbf{x}) = FT^{-1}[CSF(\mathbf{k}) \cdot FT[i(\mathbf{x})](\mathbf{k})](\mathbf{x}) = i'_{GSF}(\mathbf{x})$$
$$= GT^{-1}[GSF(\mathbf{x}, \mathbf{k}) \cdot GT[i(\mathbf{x})](\mathbf{x}, \mathbf{k})](\mathbf{x}). \quad (3)$$

Note that this expression (the relation between the Fourier and the conjoint weighting functions) is independent of the conjoint basis, so it can be applied to any general CT. The main restriction of equation (3) comes from the fact that it relates a 4D object (the conjoint weighting function) to a 2D object (the CSF). The calculation of the GSF from the CSF, using equation (3), implies the spatial independence of the GSF coefficients. In fact, as the CSF characterization requires homogeneity (spatial invariance) of the system, it does not include the possibility that the system response to a particular spatial frequency varies spatially. Nevertheless, taking into account that spatial dependence is the advantage of the GSF, as this characterization assigns several coefficients to each frequency from a stimulus of that frequency situated at different spatial position, we should include the spatial dependence effects. This can be done introducing a different attenuation over the coefficients corresponding to the same frequency but with different spatial positions in order to get a spatially variant point spread function of the system.

For all these reasons, it is apparent that equation (3) will only provide a first approximation to the GSF. The GSF obtained from equation (3) will determine an attenuation dependent on the frequency, but uniform at a certain frequency for each spatial position. As well as the CSF used in the calculation, and its corresponding point spread function (having a validity limited to the foveal region where the response to the unit stimuli remains constant), this first approximation to the GSF is only valid if it is locally applied. Although equation (3) introduces

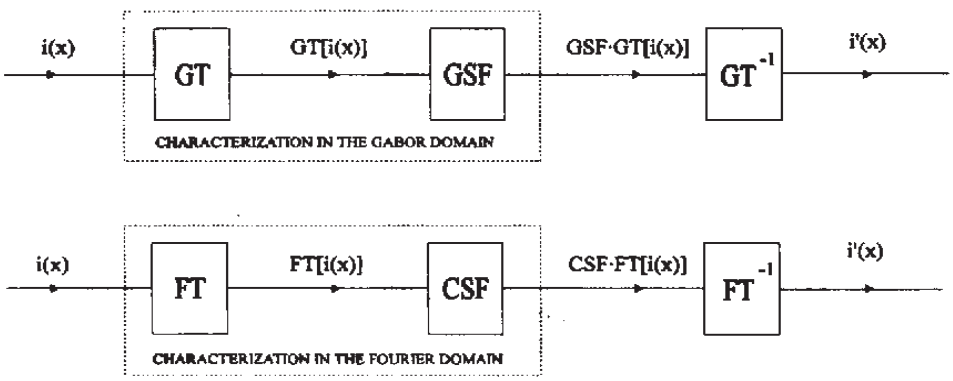

Figure 2. Obtention of a topographic signal from the encoded signal in both Gabor and Fourier representations applying the appropriate inverse transform. If the characterized system is the same, the result of both weighting processes must be the same.

local validity, this restriction can be overcome introducing a selective spatial attenuation for the coefficients of each frequency.

Having presented equation (3) and its restrictions, we shall mention the explicit relations between the CSF and the GSF. Making $i(\mathbf{x})$ in equation (3) equal to a base function $\exp(i\mathbf{k}_0\mathbf{x})$ or $g(\mathbf{x}, \mathbf{x}_0, \mathbf{k}_0)$, we can see that

$$\mathrm{GSF}(\mathbf{x}_0, \mathbf{k}_0) = \mathrm{GT}[\mathrm{FT}^{-1}[\mathrm{CSF}(\mathbf{k}) \cdot \mathrm{FT}[g(\mathbf{x}, \mathbf{x}_0, \mathbf{k}_0)](\mathbf{k})](\mathbf{x})](\mathbf{x}_0, \mathbf{k}_0), \qquad (4\,a)$$

$$\mathrm{CSF}(\mathbf{k}_0) = \mathrm{FT}[\mathrm{GT}^{-1}[\mathrm{GSF}(\mathbf{x}, \mathbf{k}) \cdot \mathrm{GT}[\exp(i\mathbf{k}_0\mathbf{x})](\mathbf{x}, \mathbf{k})](\mathbf{x})](\mathbf{k}_0), \qquad (4\,b)$$

if it is normalized. The GSF of equation (4 *a*), as mentioned above, does not involve system inhomogeneities, and it will have a local validity restricted to the region where the CSF, from which it is calculated, is valid. This problem can be solved by introducing spatial selectivity *a posteriori*.

If a general GSF, including the system inhomogeneities, is employed to calculate the CSF from equation (4 *b*), those inhomogeneities will be averaged in the calculation. Since a filter defined in a 4D domain is projected into a 2D domain, thereby all the inhomogeneities present in the 2D removed domain are averaged. This fact implies a foveal CSF undervaluation and an extra-foveal CSF overvaluation. To avoid this average over very different areas, we can calculate local CSFs from the spread function of the system for a certain area, using the equation

$$\mathrm{CSF}_{\mathbf{x}_0}(\mathbf{k}) = \mathrm{FT}[\mathrm{GT}^{-1}[\mathrm{GSF}(\mathbf{x}, \mathbf{k}) \cdot \mathrm{GT}[\delta(\mathbf{x} - \mathbf{x}_0)](\mathbf{x}, \mathbf{k})](\mathbf{x})](\mathbf{k}). \qquad (5)$$

In short, equations (4 *a*) and (5) allow us to make the GSF calculation (which does not include spatial attenuation) and the CSF calculation (with validity in the proximity of $\mathbf{x}_0$) from knowledge of the CSF and GSF, respectively.

As we can see, equations (4 *a*) and (5) are independent of the basis $\{g(\mathbf{x}, \mathbf{x}', \mathbf{k})\}$ chosen. This fact provides a certain freedom in basis selection, and then the characteristics of the visual system detection mechanisms [5–7] can be considered to a greater or lesser degree. Thus, in addition to logical dependence on the CSF, the concrete values of the GSF will be dependent on the base chosen for performing the transform.

This global-to-local drawback inherent in any 2D to 4D projection would be present in any other conjoint representation, but, as stated above, the expressions (4 *a*) and (5) are generalizable to any other linear CT, such as wavelet transforms, just by changing GT by the proper CT and making use of the proper basis (wavelets or any kind of windowed sinusoids), so the problem is equally overcome.

5. Determination of the 4D GSF from a 2D CSF

Three things are required for calculating the GSF according to equation (4 *a*):

- the Gabor's channels model: a set of base functions over which the decomposition of the signal should be carried out,
- the algorithm for calculating the GT with the chosen basis,
- experimental data about the weights in the Fourier domain.

The model of Gabor's channels employed will have to include the following properties of the visual system channels:

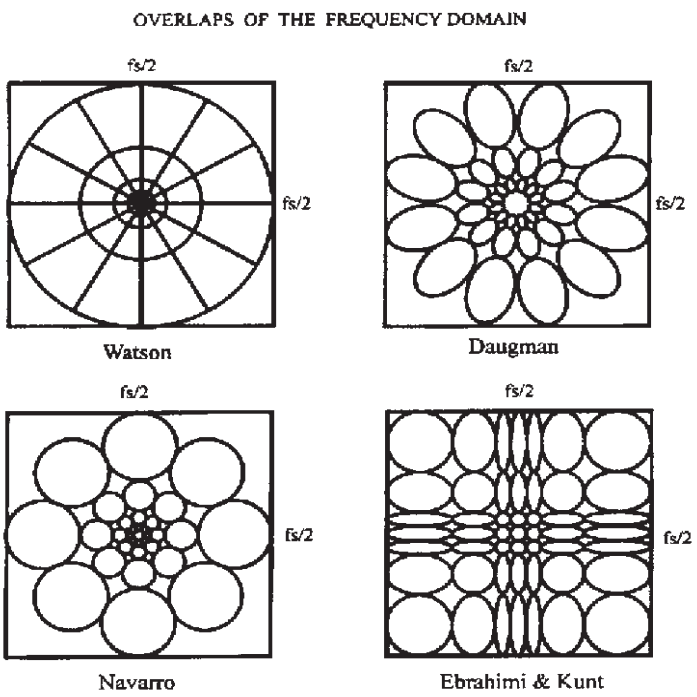

Figure 3. Different models to overlap the frequency domain with the spectra of the base functions (f_s is the sampling frequency).

- an approximately constant width in orientation (about 30°),
- a frequency width of about 1 octave,
- four or five frequency tuning mechanisms with sensitivity maximums separated by octaves.

A rigorous reproduction of these characteristics will lead us to propose an overlap of the frequency space similar to those proposed by Daugman [13], Watson [17, 18] and Navarro and Tabernero [26] (see figure 3).

We have chosen the separable base functions of Ebrahimi and Kunt [28] because, although they do not strictly fit the physiological data, they reflect their essential properties: the overlap is more compact in the low-frequency zone, the frequency width increases with the frequency, and the separation between central frequencies is also about 1 octave. Moreover, this overlap implies a lower computational cost than other algorithms, since the calculation of GT and GT^{-1} is reduced to a matrix product.

In any case, in this paper the algorithm for the GT calculation and the basis model employed are only tools and, therefore, their properties are not essential aspects of our discussion, since our main aim is to obtain the GSF weights in the Gabor domain. To do this we merely use a certain base and algorithm to apply equations (4 a) and (5). Consequently, the choice of a certain model, perhaps not the most appropriate, does not disminish the validity of the reasoning.

Using a separable basis, the functions $g_{kl}(x, y)$, defined in a 2D discrete domain of $N \times N$ points, can be written as an outer product of the functions $g_k(x)$ and $g_l(y)$ defined in a 1D domain of N points. That is:

$$[g_{kl}(x,y)] = [g_l(y)]^{[g_k(x)]}, \tag{6}$$

and, therefore, the discrete linear combination analogous to equation (1),

$$f(x) = \sum_{k,l} C_{kl} g_{kl}(x,y), \tag{7}$$

has a matrix expression

$$\mathbf{f} = \mathbf{G}_1 \mathbf{C} \mathbf{G}_2, \tag{8}$$

where $\mathbf{f}$ is the matrix of image points, the columns (rows) of the matrix $\mathbf{G}_1$ ($\mathbf{G}_2$) have as elements the 1D functions g_i, and the matrix $\mathbf{C}$ has as elements the coefficients that control the contribution of each $g_{ij}(\mathbf{x})$ in $f(\mathbf{x})$.

To obtain the GT of a function $\mathbf{f}$ with respect to a separable base implies finding the matrix $\mathbf{C}$, so that the mean square error (mse) is minimized:

$$\text{mse} = \|\mathbf{f} - \mathbf{G}_1 \mathbf{C} \mathbf{G}_2\|^2. \tag{9}$$

This kind of minimum square problem has the solution [36]

$$\mathbf{C} = \mathbf{V}_1 (\mathbf{S}_1^{\mathrm{T}})^{-1} \mathbf{U}_1^{\mathrm{T}} \mathbf{f} \mathbf{V}_2 (\mathbf{S}_2^{\mathrm{T}})^{-1} \mathbf{U}_2^{\mathrm{T}}, \tag{10}$$

where the matrices $\mathbf{U}_i, \mathbf{S}_i$ and $\mathbf{V}_i$ arise from the decomposition in singular values of the matrices $\mathbf{G}_i$. Thus, once a basis is selected, and the matrices $\mathbf{G}_i, \mathbf{U}_i, \mathbf{S}_i$ and $\mathbf{V}_i$ are calculated, the calculation of GT and GT^{-1} is reduced to computing the matrix products (10) and (8), respectively.

In this representation, the GSF filter will be given by a matrix with the same dimensions as $\mathbf{C}$, so that every coefficient GSF_{ij} acts on every coefficient C_{ij} of the GT of the image $\mathbf{f}$, in such a way that the filtered image $\mathbf{f}'$ will be

$$\mathbf{f}' = \mathbf{G}_1 \cdot \mathbf{GSF}^* \mathbf{C} \cdot \mathbf{G}_2, \tag{11}$$

where the dot symbol $\cdot$ represents the usual matrix product and $*$ is the element by element product of the GSF matrix and $\mathbf{C}$:

$$(\mathbf{GSF}^* \mathbf{C})_{ij} = \mathrm{GSF}_{ij} C_{ij}. \tag{12}$$

The space–frequency meaning of every coefficient C_{ij} or GSF_{ij} depends on how the 1D functions g_i are organized in the matrices $\mathbf{G}_i$. In our case, the base functions $g_{kl}(\mathbf{x})$ cover the frequency space as in the Ebrahimi and Kunt [28] model. The covering of the spatial domain by functions of a given frequency (not well clarified in [28]) is performed by imposing a constant overlapping, independent of the frequency, of the contiguous functions. In this manner, the low-frequency functions (of narrow spectrum and, therefore, large spatial width) are very separate in the spatial domain, so that it is covered by a few of these functions, whereas the high-frequency functions (of wide spectrum and, therefore, very spatially localized) are very close, requiring a greater number of functions by unit of area to cover the spatial domain.

Our model uses a basis with seven central frequencies in each direction: $3f_s/8, f_s/6, f_s/18, 0, -f_s/18, -f_s/6, -3f_s/8$ (f_s being the sampling frequency), i.e.

49 different frequencies and as many spatial positions as necessary to satisfy the imposed overlapping conditions. To determine an overlapping value, the criterion was the achievement of a perfect reconstruction in developing the GT and GT^{-1}. (As shown in figure 1, our model consists in assuming a *complete* encoding followed by a filtering process).

In our case, an overlapping of 85% was imposed in order to get reconstructions with a negligible error. It is apparent that the selection of a different covering of the frequency domain could perhaps have diminished the percentage of overlapping needed, but, as we said before, our goal is to use the Gabor channels model as a tool and not to optimize it.

The matrix $\mathbf{G}_1$ (or $\mathbf{G}_2$) is constituted by submatrices of columns (rows) corresponding to the different frequencies, from the most negative ones on the left (above) to the most positive ones on the right (below). Inside each of these submatrices, every column (row) corresponds with a different spatial position, being also arranged in a crescent from left to right (from top to bottom). This particular distribution of the 1D functions in the matrices $\mathbf{G}_1$ and $\mathbf{G}_2$ implies a determinated space–frequency meaning for every coefficient of the transform $\mathbf{C}$ or of the filter GSF (see one example of this in figure 4).

The beneficial effects of all the advantages of the GSF are obtained if the coefficients are calculated in the whole 4D domain (2D spatial domain and 2D frequency domain). We apply equation (4 *a*) using the data of CSFs evaluated in the whole 2D domain in such a way that they include the asymmetries in orientation of the system under study [37]. In particular, the experimental data supporting this paper are the CSFs of two observers [37]: JM (emmetropic) and RZ (astigmatic). Figure 5 shows the filter functions for both these observers.

The results of applying equation (4 *a*) to the data of JM, for every function $g_{kl}(\mathbf{x})$, is shown in figure 6 (*a*). As we can see, the weights are organized as a band-pass function, with maximum sensitivity for the functions with central frequency of 1·67 cpd ($f_s = 60$ cpd). The frequency resolution in the Gabor representation is lower than in the Fourier representation: Gabor functions have a large band and, therefore, the asymmetries of the Fourier weighting function are averaged in the Gabor representation. As we will see later, this fact does not mean that the information about the astigmatism is lost.

For a certain spatial frequency, no significant difference is obtained for the diverse spatial coefficients, as was expected from the analysis of the restrictions of equation (4 *a*), since the CSF assumes a spatial-invariant behaviour. Therefore, in the GSF there is an attenuation varying for the different submatrices corresponding to the different frequencies; nevertheless, a constant attenuation is found for all the coefficients of a given frequency corresponding to every spatial position of the function of that frequency.

A small difference is obtained for certain coefficients, especially for those corresponding with the functions more localized in frequency (and hence much more extended in space), this effect being stronger for the most external positions. This systematic deviation is caused by the finite character of the spatial domain considered, in such a way that a sort of spectral leakage [38] occurs. The function with larger spatial width placed on the border of the domain has non-zero values beyond the limits of the considered domain. This produces a distortion in the result of equation (4 *a*) with regard to other positions, in which the area where the function has a significant value is completely contained in the domain considered.

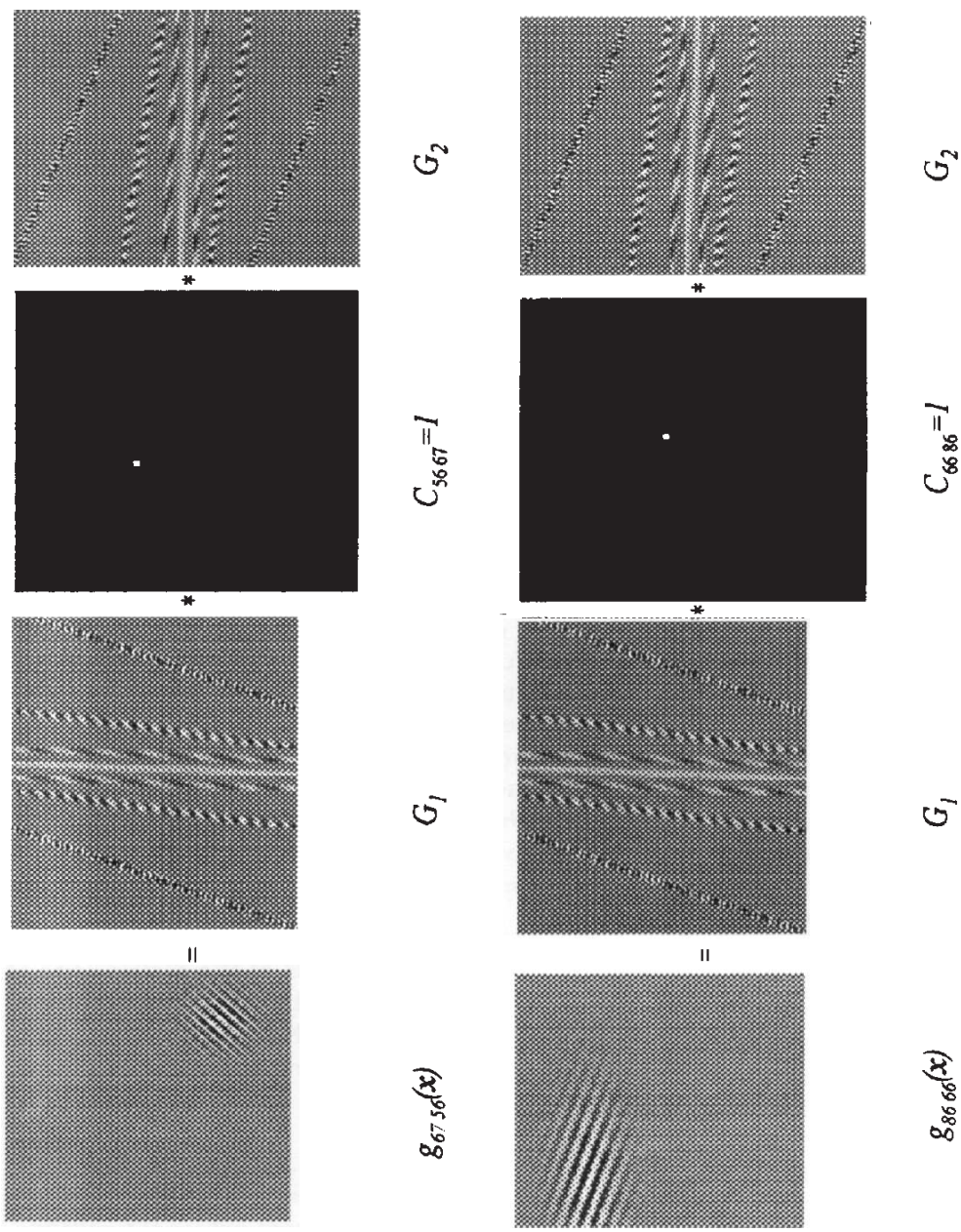

Figure 4. Two examples of the meaning of the GT coefficients: each element of the **C** matrix selects one column of $\mathbf{G}_1$ and one row of $\mathbf{G}_2$ to generate the corresponding base function. In these examples we can see how the coefficients $C_{56\,67}$ and $C_{66\,86}$ (any other elements in the matrix are zero) give rise to the functions $g_{67\,56}(\mathbf{x})$ and $g_{86\,66}(\mathbf{x})$, respectively.

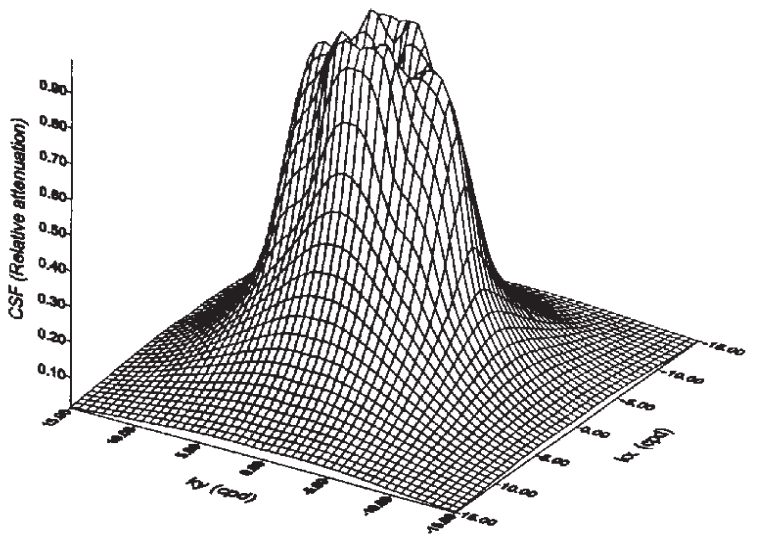

(*a*)

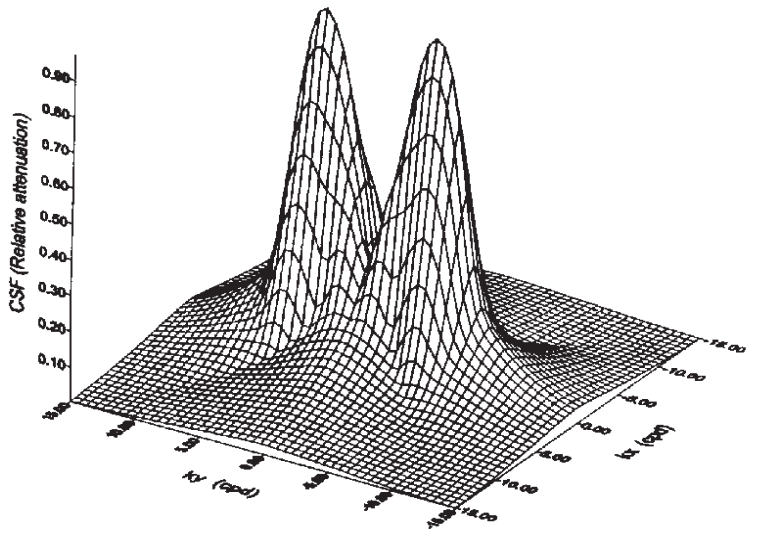

(*b*)

Figure 5. Experimental 2D CSFs of the observers. (*a*) Observer JM (emmetropic), (*b*) Observer RZ (astigmatic −3 dp 0°). Note how the revolution symmetry of the CSF breaks down in this case, favouring vertical frequencies. For details on the measurement of these functions, see [37].

These deviations are only originated by the calculation in a spatially limited domain, and therefore they are not connected at all with the system characteristics. The real value of the attenuation for these stimuli will be given by the results obtained for functions completely contained in the spatial domain.

According to all these considerations, in order to obtain the GSF from equation (4 *a*), it is necessary to calculate only the GSF_{ij} coefficients for the $g_{ij}(\mathbf{x})$ functions

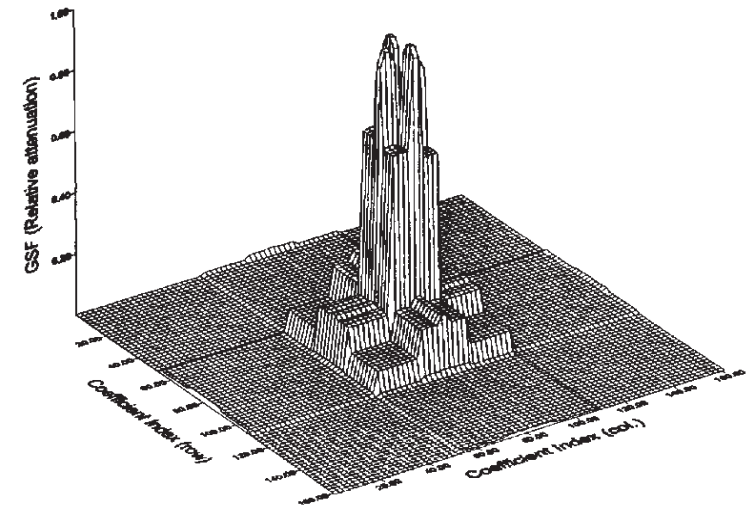

(*a*)

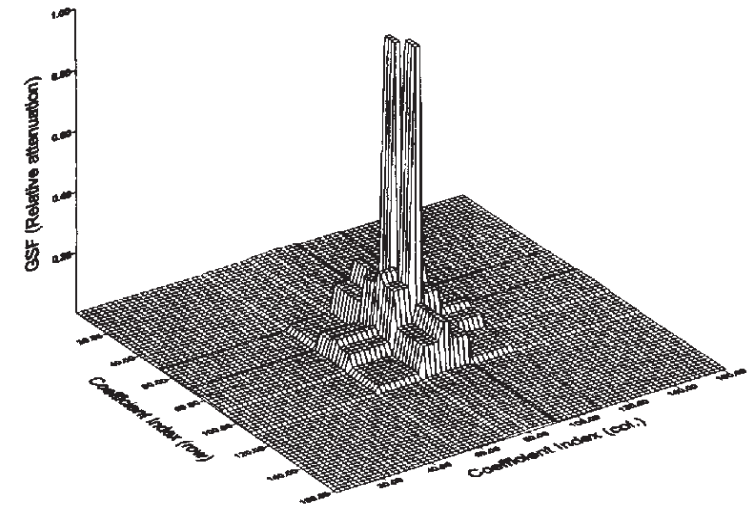

(*b*)

Figure 6. GSFs of the observers obtained from the CSFs of figure 5 by means of equation (4 *a*). The space–frequency meaning of the different coefficients is explained in the text. (*a*) Fully calculated GSF of the observer JM (emmetropic). Note the unexpected deviations of the coefficients of the border of each submatrix (the more external spatial coefficients). These small deviations are due to the finite length of the considered spatial domain. Note that the attenuation depends basically on the magnitude of **k**, but not on the orientation of the frequency vector. (*b*) Sparse calculated GSF of the observer RZ (astigmatic) avoiding the border errors (see text). It is remarkable to see the strong differences in the attenuation of the central submatrices caused by astigmatism.

placed in the centre of the spatial domain considered, avoiding, in this way, border errors and also saving a great amount of calculation. The value calculated for the central coefficient of every submatrix is extended to the rest of the submatrix coefficients to get the final GSF. Using this procedure, we obtain the filter function for the astigmatic observer (figure 6 (*b*)).

6. Equivalence between the spatially invariant GSF and the CSF in the foveal region

To demonstrate the equivalence between the computed GSFs and the CSFs from which they have been calculated, we simulate the spread function of the system and the complex image filtering by means of the GSF. Afterwards, we compare such simulations with other ones from the experimentally measured CSFs. The system spread function calculation and the complex image filtering from the experimental data of a 2D CSF were carried out according to the method presented in previous work [37] The filtered image of an object test from the GSF data was calculated using equation (11), where the matrix **C** corresponds with the GT coefficients of the object test.

Figures 7 and 8 show the results of the point spread functions (PSFs) for the two observers obtained from their GSFs (figures 7 (*b*) and 8 (*b*)), and compared with the analogous results obtained from the experimental measures of the CSFs (figures 7 (*a*)) and 8 (*a*)). As we can see, the width at half height of the PSF is adequately reproduced for both observers, as well as the PSF deformation along the x axis in the astigmatic observer's case. Although the astigmatism is not clearly manifested in the shape of the GSF because of its lower frequency resolution, this representation keeps the information about the system asymmetries in orientation.

The agreement between both characterizations is also observed in the simulations of complex object processing (figures 9 and 10). Figure 9 shows the processing of a natural image, whereas in figure 10 we employed a circular test to manifest the asymmetries in orientation. The general degradation of the original image (figure 9 (*a*)), when weighted by the GSF of the observer JM (figure 9 (*b*)) and by the CSF of the same observer (figure 9 (*c*)), is equivalent: the difference in mean square error is only about 12%. Figures 9 (*d*) and (*e*) show analogous results for the observer RZ. The difference between both results in this case is 18%. As can be observed in figure 10, the GSF reproduces well the astigmatic behaviour of the observer RZ. The horizontal borders appear much more sharply than the vertical ones, both when the image has been weighted by the GSF (figure 10 (*b*)) and when Fourier simulation is used. For the emmetropic observer (JM) we can see that the degradation appearing in the test is isotropic (figures 10 (*d*) and (*e*)).

The results demonstrate the accuracy of the assumption on which equation (4 *a*) is based, and the validity of the particular results for the GSFs of the observers JM and RZ, obtained from their CSFs in the foveal region.

7. Spatial non-homogeneities introduced in the GSF: characterization of spatially variant systems

In this section we demonstrate that it is possible to introduce spatial non-homogeneities in the GSF, so that the characterized system will have a spatially variant behaviour. To do this, we infer a simulated observer from the data of the real observers in such a way that the synthesized observer has a different

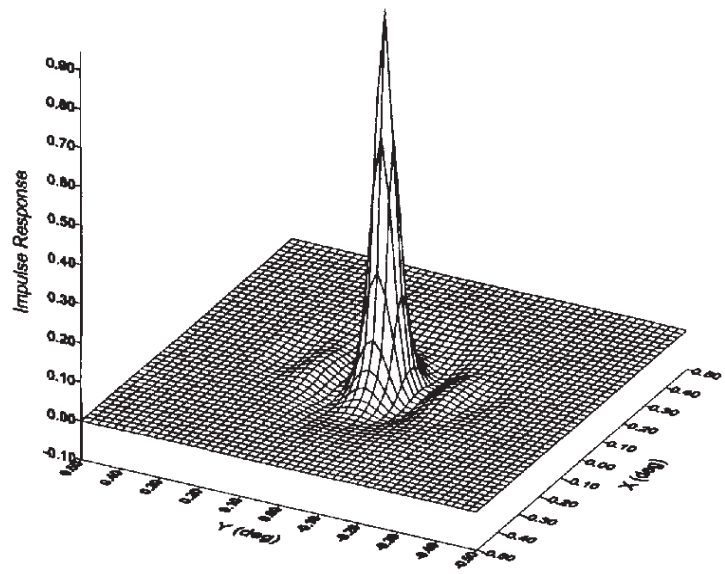

(*a*)

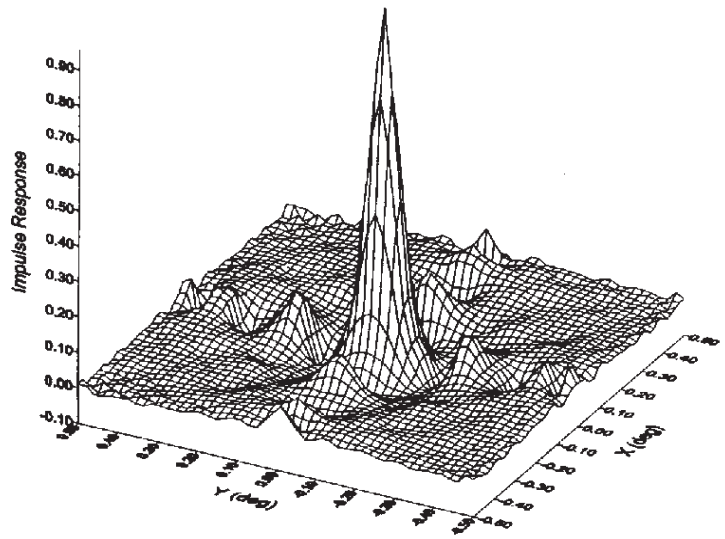

(*b*)

Figure 7. Point spread functions of the emmetropic observer obtained from (*a*) the Fourier characterization and (*b*) the Gabor characterization.

behaviour, emmetropic or astigmatic, in different spatial zones. That is, we have synthesized a non-homogeneous observer. It is qualitatively shown in this simulation how the non-homogeneities of the system can be introduced to characterize the vision in large fields. A realistic model of this type of perception would necessarily include, in a systematic form, data about the system response to different eccentricities [39, 40], which would simply imply an increment in the

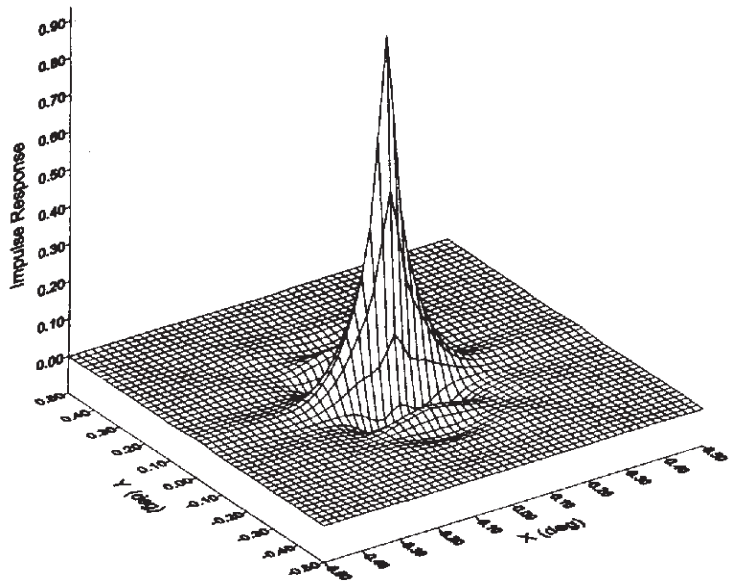

(*a*)

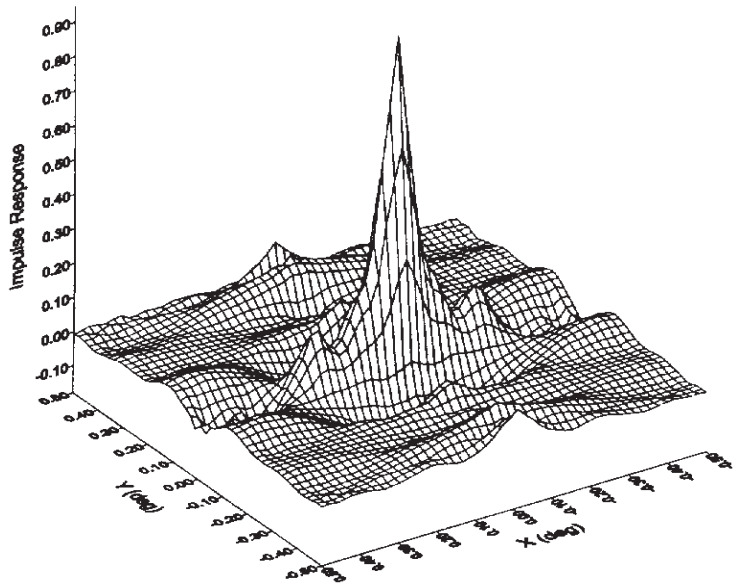

(*b*)

Figure 8. PSFs of the astigmatic observer obtained from (*a*) the Fourier characterization and (*b*) the Gabor characterization.

number of spatial positions considered for every frequency, increasing the size of the coefficients matrix of the GT.

As our purpose is only to show the potential of the characterization presented to perform this task, it will be sufficient to demonstrate that the GSF can include inhomogeneous behaviours. This fact will be examined with a synthesized example

(*a*)

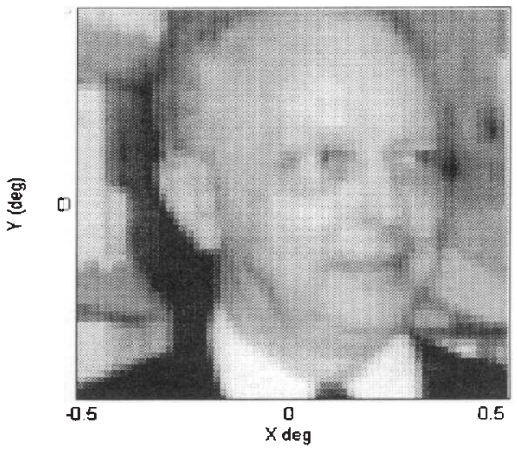

(*b*)

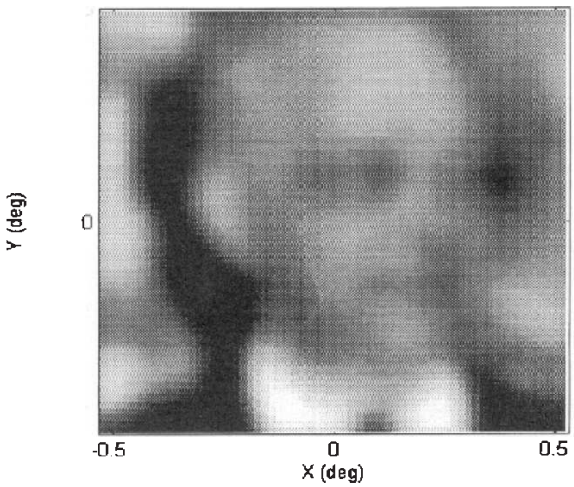

(*c*)

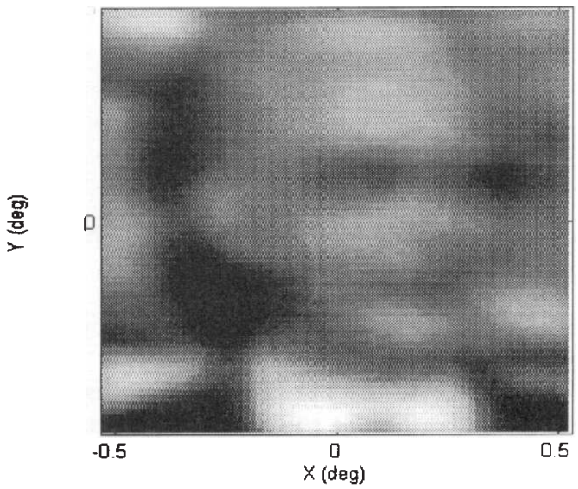

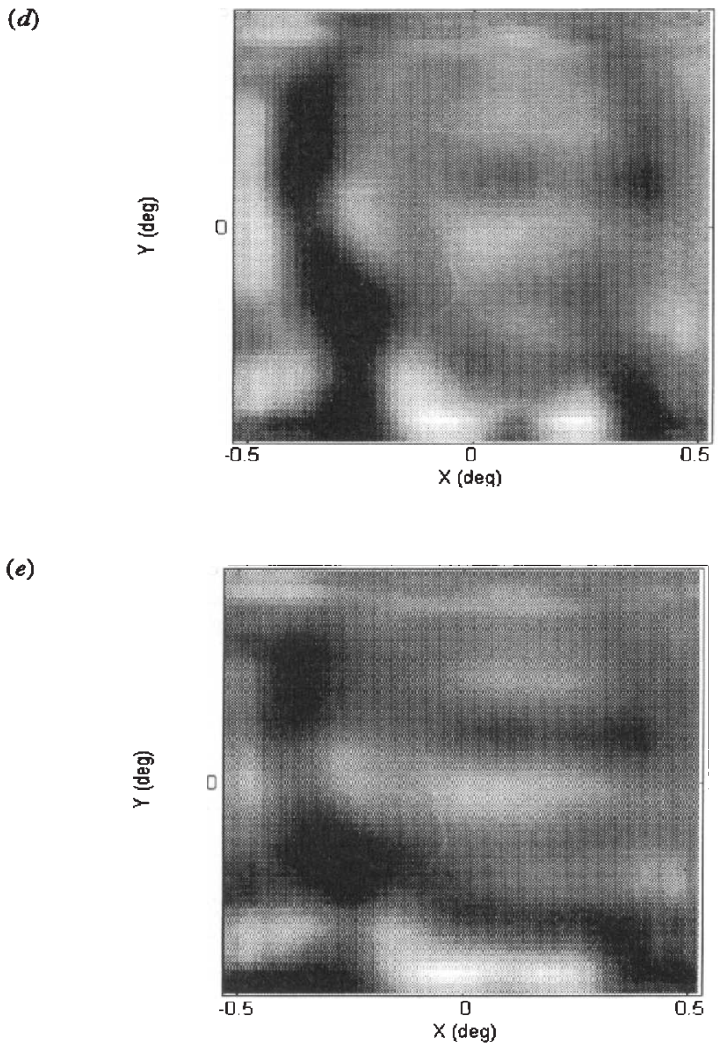

Figure 9. Natural image filtering. (*a*) Shows the original natural image (Prof. Givens 1964 photo from the Gatlinburg Conference on Numerical Algebra). (*b*) Shows the natural image weighted by the GSF of the emmetropic observer and (*c*) shows the result using the CSF. (*d*) Displays the natural image weighted by the GSF of the astigmatic observer. Note the different behaviour of both observers. The astigmatic observer blurs the vertical borders (horizontal frequencies) and relatively enhances the horizontal borders (vertical frequencies). This can be seen in both Gabor and Fourier characterizations. (*e*) shows the natural image weighted by the CSF of the astigmatic observer.

of non-homogeneity in the foveal region, which allows us to use the algorithm already developed. The introduction of spatial asymmetries means loss of uniformity in the spatial coefficients of a given submatrix of a particular frequency. In other words, it means imposing spatially varying sensitivity on every frequency component.

The weighting function of the simulated observer is generated by substituting the GSF values of the observer RZ in the spatial positions corresponding to the

(*a*)

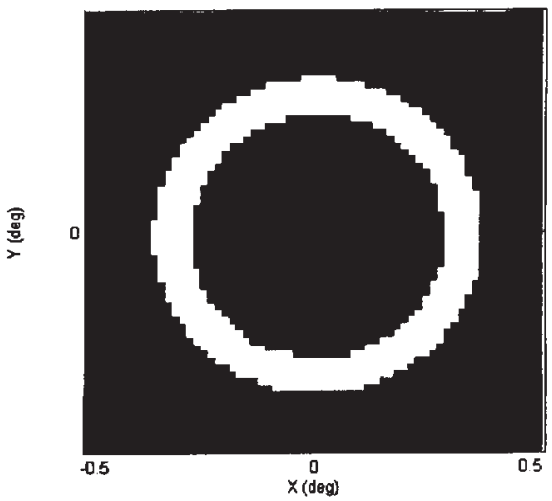

(*b*)

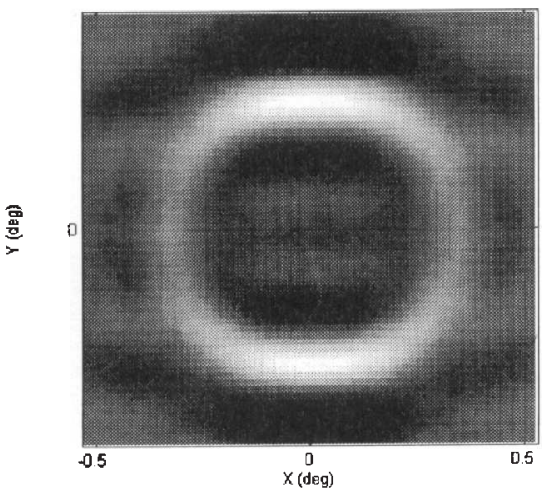

(*c*)

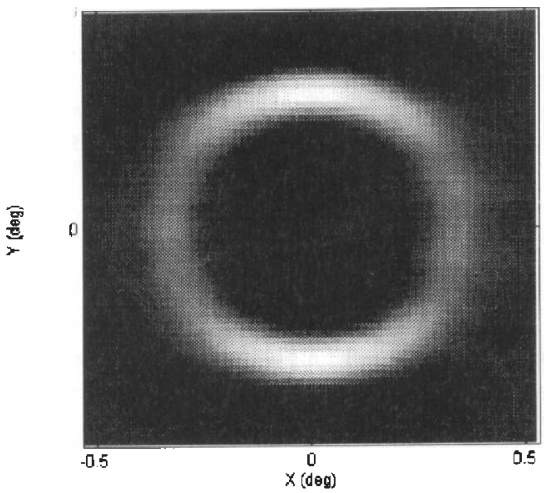

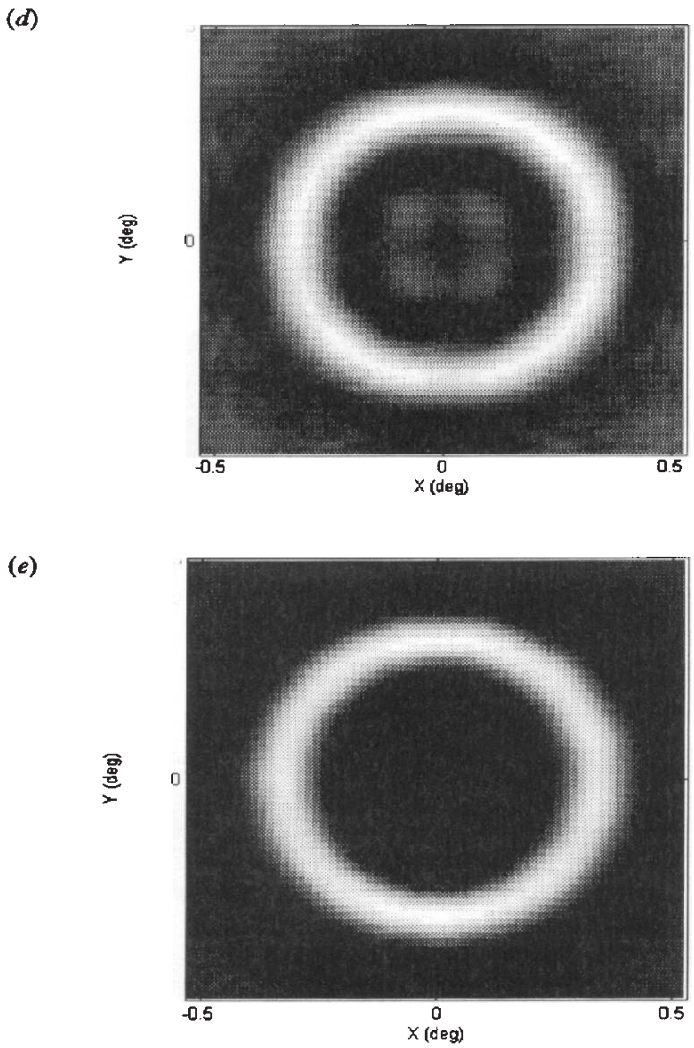

Figure 10. Circular test filtering. (*a*) Depicts the original circular test. (*b*) Shows the circular test weighted by the GSF of the astigmatic observer and (*c*) shows the analogue result using the CSF. (*d*) Displays the circular test processed by the GSF of the emmetropic observer and (*e*) shows the result in the Fourier characterization for the emmetropic observer.

upper part of the image in the GSF of the observer JM. This gives astigmatic behaviour for $y > 0$ and emmetropic behaviour for $y < 0$. The result of the synthesized weighting function is shown in figure 11, and the result of the perception simulation of the circular test in figure 12.

The different degree of astigmatism, in the different zones considered, is apparent in figure 12. The definition at the borders of the test is limited to a small angle in the upper half (strong astigmatism), while in the lower half the angular range is bigger. The transition from emmetropic to astigmatic behaviour is smooth because the differences in attenuation between spatial zones corresponding to each of the filters have been smoothed (compare figures 11 and 6). The superposition of two functions, of equal frequency, in close spatial positions and with very different

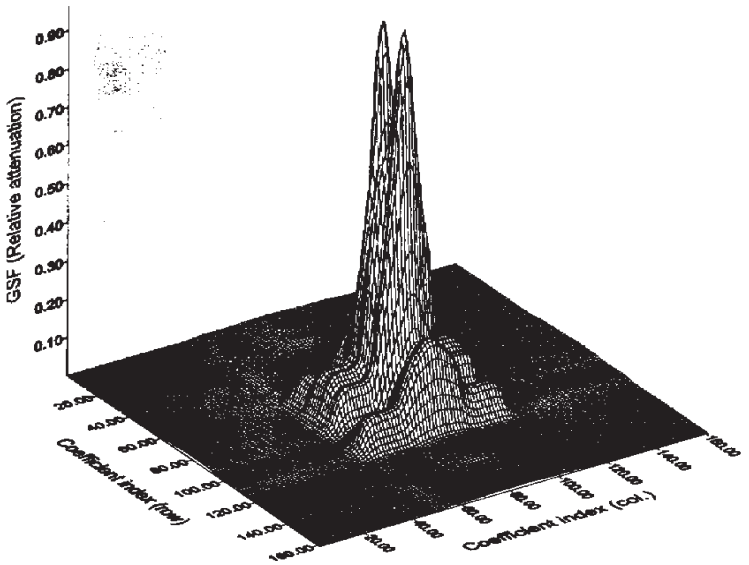

Figure 11. Synthetic GSF obtained mixing the weighting functions of figures 6 (*a*) and (*b*) in different spatial positions.

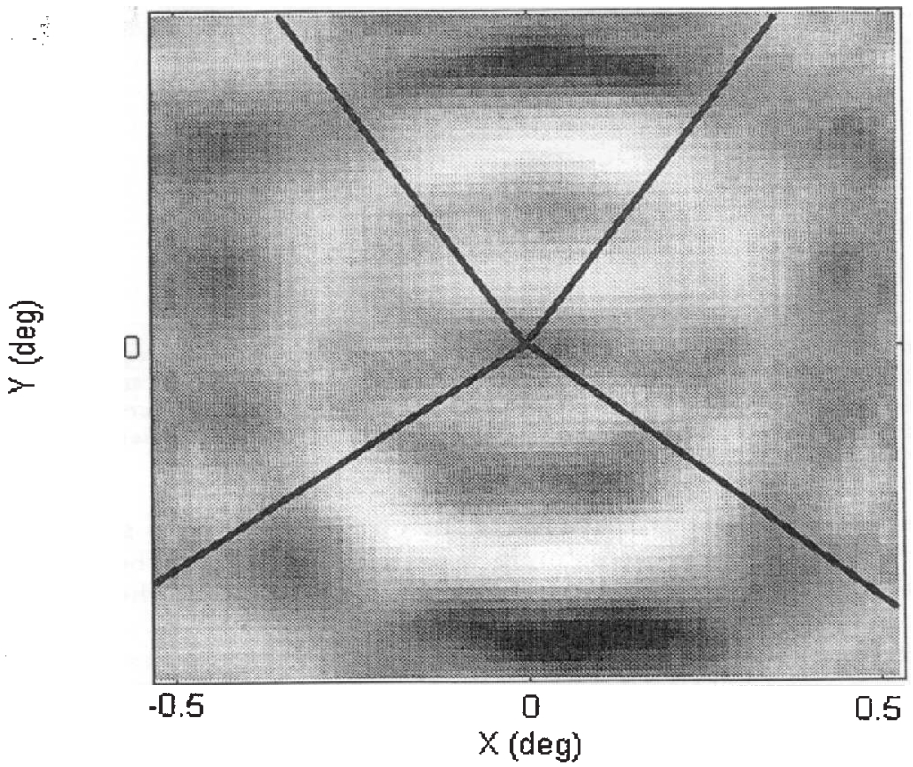

Figure 12. Circular test processed by the synthetic weighting function. Note the astigmatic behaviour in the upper half of the figure and the emmetropic behaviour in the lower half, evidenced by the difference of the angle of sharp discrimination.

attenuation, implies the existence of noise in the transition zone originated by non-cancelled oscillations due to the partial non-orthogonality of the base function of the same frequency. This fact imposes a restriction on the characterization of systems with too sharp spatial variations. This is not a problem in the visual system case where a smooth spatial variation is reported [39, 40]. In our synthetic example we must obtain a smooth variation between spatial zones with different attenuation. In this case we performed the smoothing by convolution of the synthesized filter with a Gaussian function.

This example does not attempt to be a model for the spatial variations of the visual system, but it simply manifests that such variations can be included perfectly well in a characterization such as the one presented. If the desired local Fourier weighting functions (CSF_i) are known, we can take advantage of the relation between the CSF and its analogue in the Gabor domain, the GSF (equation 4 *a*), to calculate the conjoint homogeneous weighting functions GSF_i from their Fourier equivalents CSF_i, and afterwards combine the coefficients from the different GSF_i in the desired spatial positions in order to generate the single non-homogeneous weighting function in the conjoint domain. In this way, we achieve a straight characterization of the spatially variant system: instead of applying multiple convolution kernels in different spatial positions, a single conjoint attenuation process takes into account all the non-homogeneities of the system.

To conclude, we would like to restate here that the conjoint weighting idea and the equations stated are not restricted by the selection of either the basis or the transformation. Therefore, it is also possible to work on defining a weighting function according to either another basis or another space/spatial frequency linear transformation, which may be considered to be more suitable or to be a better representation of the physiology of vision.

References

[1] Kersten, D., 1987, *J. opt. Soc. Am.* A, **4**, 2395.
[2] Gonzalez, R. C., and Wintz, P., 1987, Digital Image Processing (Reading, MA: Addison-Wesley), chap. 6.
[3] Field, D., 1987, *J. opt. Soc. Am.* A, **4**, 2379.
[4] Campbell, F. W., and Green, D., 1965; *J. Physiol.*, **181**, 576.
[5] de Valois, R. L., Albrecht, D. G., and Thorell, L. G., 1982, *Vision Res.*, **22**, 545.
[6] Webster, M. A., and de Valois, R. L., 1985, *J. opt. Soc. Am.* A, **2**, 1124.
[7] Marcelja, S., 1980, *J. opt. Soc. Am.*, **70**, 1297.
[8] Daugman, J. G., 1980, *Vision Res.*, **20**, 847.
[9] Daugman, J. G., 1983, *IEEE Trans. Syst., Man, Cybern.*, **13**, 882.
[10] Daugman, J. G., 1984, *Vision Res.*, **24**, 891.
[11] Harvey, L. O., and Doan, V. V., 1990, *J. Opt. Soc. Am.*, **7**, 116.
[12] Daugman, J. G., 1985, *J. opt. Soc. Am.* A, **2**, 1160.
[13] Daugman, J. G., 1988, *IEEE Trans. Acoust., Speech, Signal Process.*, **36**, 1169.
[14] Porat, M., and Zeevi, Y. Y., 1988, *IEEE Trans. Pattern Anal. machine Intell.*, **10**, 452.
[15] Field, D. J., Hayes, A., and Hess, R. F., 1993, *Vision Res.*, **33**, 173.
[16] Watson, A. B., 1983, *Physical and Biological Processing of Images*, edited by Braddick and Sleigh (Berlin: Springer), pp. 100–114.
[17] Watson, A. B., 1987, *Comput. Vision Graph. Image Process.*, **39**, 311.
[18] Watson, A. B., 1987, *J. Opt. Soc. Am.* A, **4**, 2401.
[19] Stork, D. G., and Wilson, H. R., 1990, *J. opt. Soc. Am.* A, **7**, 1368.
[20] Daubechies, I., 1988, *Commun. pure appl. Math.*, **41**, 909.

[21] MALLAT, S. G., 1989, *Trans. Am. math. Soc.*, **315**, 69.
[22] CHUI, C. K., 1992, *An Introduction to Wavelets* (London: Academic Press).
[23] MALLAT, S. G., 1989, *IEEE Trans. Pattern Anal. machine Intell.* **7**, 674.
[24] Special Issue on Wavelet Analysis, 1992, *IEEE Trans. Inf. Theory*, **38** (2).
[25] GABOR, D., 1946, *JIEE*, **93**, 429.
[26] NAVARRO, R., and TABERNERO, A., 1991, *Multidim. Sys. Signal Process.*, **2**, 421.
[27] BASTIAANS, M. J., 1982, *Optica Acta*, **29**, 1223.
[28] EBRAHIMI, T., and KUNT, M., 1991, *Opt. Eng.*, **30**, 873.
[29] COHEN, A., and FROMENT, J., 1992, *Wavelets and Applications*, edited by Y. Meyer (Berlin: Springer), pp. 181–206.
[30] ANTONINI, M., BARLAUD, M., and MATHIEU, P., 1992, *Wavelets and Applications*, edited by Y. Meyer (Berlin: Springer), pp. 160–174.
[31] BOVIK, A. C., CLARK, M., and GEISLER, W. S., 1990, *IEEE Trans. Pattern Anal. Machine Intell.*, **12**, 55.
[32] GAUDART, L., CREBASSA, J., and PETRAKIAN, J. P., 1993, *Appl. Optics*, **32**, 4119.
[33] LANDY, M. S., and BERGEN, J. R., 1991, *Vision Res.*, **31**, 679.
[34] POLAT, U., and SAGI, D., 1994, *Vision Res.*, **34**, 73.
[35] SALEH, B. E. A., 1982, *Applications of Optical Fourier Transforms*, edited by H. Stark (New York: Academic Press), chap. 10.
[36] PRESS, W. H., FLANNERY, B. P., TEUKOLSKY, S. A., and VETTERLING, W. T., 1992, *Numerical Recipes in C: the Art of Scientific Computing* (Cambridge: Cambridge University Press), chap. 2.
[37] MALO, J., FELIPE, A., LUQUE, M. J., and ARTIGAS, J. M., 1994, *J. Optics*, **25**, 93.
[38] PROAKIS, J. G., and MANOLAKIS, D. G., 1992, *Digital Signal Processing. Principles, Algorithms and Applications* (New York: Macmillan), chap. 6, p. 450.
[39] KELLY, D. H., 1985, *Vision Res.*, **25**, 1895.
[40] NAVARRO, R., ARTAL, P., and WILLIAMS, D. R., 1993, *J. opt. Soc. Am.* A, **10**, 201.